Molecular Crystals and Liquid Crystals Incorporating Nonlinear Optics

Publication details, including instructions for authors and subscription information:
http://www.tandfonline.com/loi/gmcl17

A Non-Aqueous Thermoreversible Lyotropic Gelling System: Characterization of Gels and Xerogels from Low Molecular Weight Steroid Derivatives

P. Terech [a b]

[a] Centre d'Etudes Nucléaires de Grenoble, DRF/Physique du Solide, Groupe de Physico-Chimie Moléculaire, 85X, 38041, Grenoble Cedex, France

[b] Institut Laue-Langevin, 156X, 38042, Grenoble Cedex

Version of record first published: 22 Sep 2006.

To cite this article: P. Terech (1989): A Non-Aqueous Thermoreversible Lyotropic Gelling System: Characterization of Gels and Xerogels from Low Molecular Weight Steroid Derivatives, Molecular Crystals and Liquid Crystals Incorporating Nonlinear Optics, 166:1, 29-41

To link to this article: http://dx.doi.org/10.1080/00268948908037136

Mol. Cryst. Liq. Cryst., 1989, Vol. 166, pp. 29–41
Reprints available directly from the publisher
Photocopying permitted by license only

Printed in the United States of America

A Non-Aqueous Thermoreversible Lyotropic Gelling System: Characterization of Gels and Xerogels from Low Molecular Weight Steroid Derivatives

P. TERECH†

Centre d'Etudes Nucléaires de Grenoble, DRF/Physique du Solide, Groupe de Physico-Chimie Moléculaire, 85X, 38041 Grenoble Cedex, France

(*Received January 4, 1988; in final form March 2, 1988*)

The gel to xerogel transformation of a steroid/cyclohexane gelling system is studied by optical microscopy, differential scanning calorimetry (DSC) and infrared (IR) spectroscopy. Nematic-like birefringent domains are observed for systems of increasing concentrations. It is demonstrated that the molecular organization is different in the solution, gel, xerogel and crystalline states. In particular, when the temperature is increased from the solid xerogel state, a phase transition to a crystalline state occurs before the melting to the isotropic liquid. The xerogel structure can only be obtained through a gelation route from solutions. Different behaviors for two steroid derivatives with different polarities are compared with thermoreversible polymeric gelling systems.

INTRODUCTION

Various low molecular weight compounds are known to form gel phases in adequate solvents. As example, in aqueous media, deoxycholate bile salts are frequently studied[1,2] with respect to their biological applications. In organic solvents, a typical example is 12-hydroxy-octadecanoic acid[3,4] and derivatives of applied interest in industrial lubricating greases[5] and cosmetics. Despite the large difference in molecular size between such compounds and some natural or synthetic polymers such as collagen,[6] agarose[7] and polystyrene,[8] there are numerous analogies in some macroscopic behaviors of the related gel states. These are linked to the thermodynamical properties of a dispersion of fibres in a solvent: the ability to phase separate in poor solvents, to become reversibly turbid in various experimental conditions, to compete with a crystallization process in some solvents and to exhibit swelling and deswelling behaviors. Therefore, the distinction between small molecules and polymeric thermoreversible systems tends to smear out when micronic

†Present address: Institut Laue-Langevin, 156X, 38042 Grenoble Cedex.

scale properties are considered. In this study, we are interested in the structural modifications which occur when a gel sample is submitted to solvent evaporation. The resulting solid state is called xerogel or dried gel. Besides the interest of the thermodynamic background underlying the fibre reorganization during solvent evaporation, the applied point of view is also concerned. Indeed, for about fifteen years, the so-called sol-gel process is widely used for obtention of special films, coatings and ceramics mainly from inorganic[9] but also from organic systems.[10]

Here we are concerned with steroid derivatives[11] gel forming in cyclohexane and various saturated hydrocarbons. Consistent structural, kinetic and thermodynamic informations have already been obtained concerning the gel state and the related sol-gel transition. In the following we summarize the results of use in the present paper. We have shown that the kinetic of gelation[12] could be varied in a range of characteristic times spreading from quite instant phenomenon to a several hours delay reactions. The driving force of aggregation kinetics is strongly dependent upon the steroid concentration ratio c/c* where C* refers to the critical solution/gel threshold at a given temperature.[12] The gelation threshold itself has been studied with a magnetic sphere rheometer.[13,14] A detailed structural study of the gel network in cyclohexane by electron microscopy (freeze etching method[15]) and small angle neutron scattering (SANS) experiments[16] provided the following picture of the native gel network. It is constituted by an assembly of very long entangled 9.5 nm diameter chiral filaments made up with two coiled finer filaments. The solid xerogel state obtained by cyclohexane evaporation has been studied at room temperature by transmission electron microscopy (TEM[17]). Fibres are in this case about 3 times broader and have very enhanced helical superstructures (mean pitch ~60 nm).

In this paper, we present results obtained by optical microscopy (OM), differential scanning calorimetry (DSC) and infrared absorption (IR) spectroscopy concerning the gel to xerogel transformation. At various stages of the paper, some analogies with thermoreversible polymeric gels are pointed out.

EXPERIMENTAL

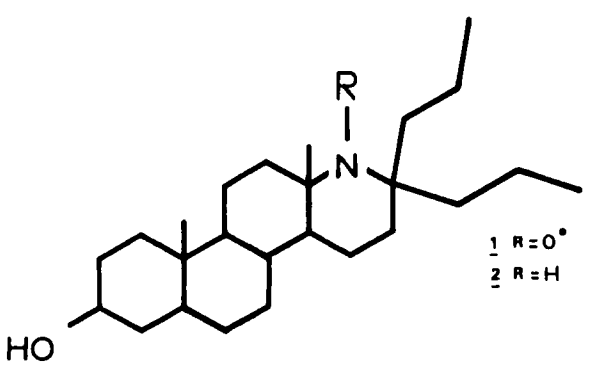

Compounds 1,2 are synthetized according to Reference 11. Pure crystalline powders are obtained from non-gelling solvent as ethyloxide. Gold label Aldrich cyclohexane

is used without further purification. Mother gelling solutions are prepared by dissolving the steroid in hot cyclohexane under vigorous shaking. Gels are obtained when the temperature is decreased. Stability of the gel phases is very good in cyclohexane in that the samples remain unchanged during several years. The situation is different when other hydrocarbons are used. In these cases, the obtained gel phases from compound 1 for instance, compete with a temperature dependent crystallization process which finally destroys the gel phase within a few minutes for heptan to several hours for decalin. In this paper, only experiments with cyclohexane samples are presented in detail. A slightly turbid aspect is obtained from initial transparent gel ($C < 2.10^{-2}$ M) when temperature is decreased. The same observation can be made at room temperature for concentrated gels ($C > 6.10^{-2}$ M) on variable aging time delays.

Xerogels are obtained by slow evaporation of cyclohexane at room temperature under atmospheric or slightly reduced pressures. A Perkin Elmer DSC-2C calorimeter is used with nontightly-sealed 20 μL aluminium cells. Optical observations are made under crossed polars either on a Reichert Thermo Diavar or Nachet N5400 microscopes. Infrared spectra are obtained from a Beckmann 4540 double beam spectrometer using for solutions and gel states variable width cells with fluorine windows for compensation of solvent absorption. Polycrystalline powder spectra are obtained as usual from a KBr powder mixture while the xerogel spectrum is recorded from the solid xerogel deposit onto one window.

RESULTS

Previous mentioned electron microscopy results show important structural modifications of the filamentary network in the dried gel and suggest that the xerogel should be considered as a new material.

Firstly, the pure solid xerogel state is studied to characterize these modifications as a new mesomorphic state, DSC and OM are complementary techniques to study these phase transitions while IR spectroscopy is used to insight the local order changes.

Secondly, the whole process of xerogel obtention by solvent evaporation is observed by OM. At various stages of the study the paramagnetic compound 1 and diamagnetic compound 2 have slightly different behaviors which are noted.

1. Xerogels and crystalline powders

DSC analysis. DSC is used to differentiate the thermal behavior of a xerogel from the corresponding crystalline powder. Figure 1 shows the thermograms for the paramagnetic nitroxide compound 1 while Figure 2 concerns the diamagnetic compound 2, both derivatives giving gels but in slightly different concentration ranges. Indicative values of the concentration limit C* (293 K) for gelation at room temperature are respectively 1.05×10^{-2} M[18] and about 2.0×10^{-2} M.

Crystalline powders of both compounds 1 and 2 (Figures 1a and 2a) exhibit only sharp endothermic peak (I) for their melting first order transition. For these samples

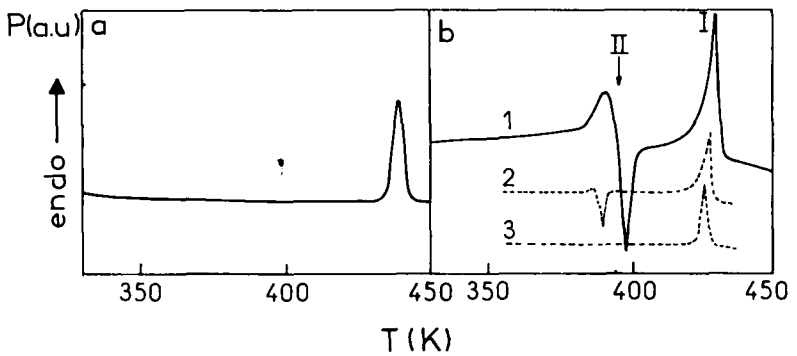

FIGURE 1 DSC thermograms for compound 1 samples. Ordinates are power in arbitrary units: (a) crystalline powder; (b) xerogel I, II refer to transitions as described in text; (b1) xerogel, heating rate = 10 K min^{-1}; (b2) xerogel, heating rate = 2.5 K min^{-1}; (b3) xerogel annealed at $T_{II} < T < T_I$, heating rate = 10 K min^{-1}.

no other premelting transitions have been detected even when rapid heating rates are used in order to visualize the small enthalpies. Temperatures and enthalpies are summarized in Table I (compound 1) and Table II (compound 2). By contrast, xerogels give additional peaks. In the case of nitroxide, the additional complex peak (II) is composed of an endothermic part immediately followed by an exothermic process and finally by the endothermic melting transition (I). I, II, III subscripts of figures and tables refer to the temperature extremas† of the above sequence numbered from the melting transition. Decreasing the heating rate gives a less pronounced complex peak II (Figure 1b2). Enthalpic balance of the additional

†Onset temperatures have been determined only for the narrow peaks of the transition crystal to liquid and were 2 degrees below the corresponding extrema temperatures.

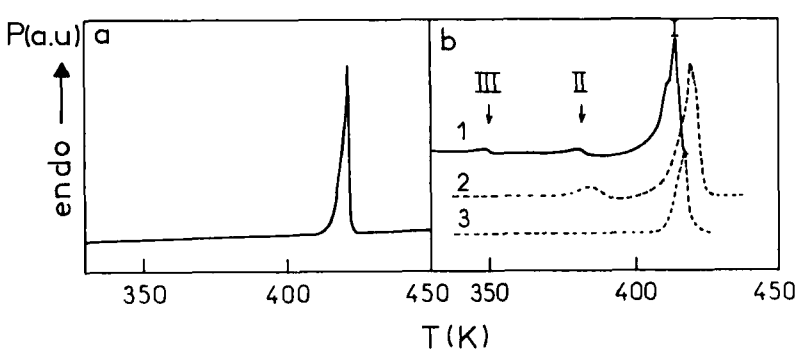

FIGURE 2 DSC thermograms for compound 2 samples. Ordinates are power in arbitrary units: (a) crystalline powder; (b) xerogel I, II, III refer to transitions as described in text; (b1) xerogel, heating rate = 10 K min^{-1}; (b2) xerogel annealed at $T_{III} < T < T_{II}$, heating rate = 20 K min^{-1}; (b3) xerogel annealed at $T_{II} < T < T_I$, heating rate = 20 K min^{-1}.

TABLE I

Steroid compound 1. Calorimetric analysis of crystalline and xerogel solid samples. I, II refer to peaks as assigned in Figure 1. Temperatures are in Kelvin.

Sample	Peaks	
	II	I
Crystalline powder (onset)	—	436 (8.05 kCal mole^{-1})
Xerogel (extremas)	391.5/398.4	428.5 (5.8 kCal mole^{-1})

complex peak II varies from 0.09 kCal mole^{-1} to 0.8 kCal mole^{-1} for a given heating rate. This peak is a characteristic signature of the solid xerogel state since the corresponding transition(s) is (are) irreversible in the solid state whatever the stop temperature of the heating process above T_{II} (Figure 1b3).

In the case of the amine compound 2 there are, in addition to the melting transition I, two peaks (Figure 2b1) which appear as essentially endothermic transitions (II and III). The first peak (III) disappears when the sample is annealed at a temperature $T_{III} < T < T_{II}$ (Figure 2b2). For the second peak T_{II} the shape and amplitude are different of that for compound 1 since no sharp exothermic transition can be detected. But like compound 1 transition(s) II is (are) irreversible in the solid state when the sample is annealed at a temperature $T_{II} < T < T_I$ (Figure 2b3). Table II summarizes the results.

Optical microscopy. Calorimetric experiments are clarified by microscopic observations under crossed polarizers of xerogel samples submitted to an identical heating rate process used in the above described DSC experiments. The following sequence is observed:

$$\text{dark or slightly birefringent} \xrightarrow{T_c} \text{crystallization} \xrightarrow{T_M} \text{isotropic liquid}$$

Table III sums up the corresponding transition temperatures for the two compounds 1,2 and specifies the different crystallization figures observed.

TABLE II

Steroid compound 2. Calorimetric analysis of crystalline and xerogel solid samples I, II, III refer to peaks as assigned in Figure 2. Temperatures are in Kelvin.

Sample	Peaks		
	III	II	I
Crystalline powder (onset)	—	—	418.3 (10.2 kCal mole^{-1})
Xerogel (extremas)	352.5	383.3	417.8 (7.4 kCal mole^{-1})

TABLE III

Optical characterization of the thermal behavior of xerogels from compounds 1 and 2. T_C and T_M refer to crystallization and melting temperatures respectively.

	T_C(K)	T_M(K)	Crystallization patterns
Compound 1	392	431.5	radial growth (spherulitic)
Compound 2	379	420	needle-like

Infrared spectroscopy. Structural distinction between the xerogel and crystalline powder is achieved by IR spectroscopy. Figure 3 shows the characteristic spectra in the O—H valency vibration frequency region for compound 1 samples. The crystalline powder spectrum exhibits (Figure 3b) an intense and broad line at 3470

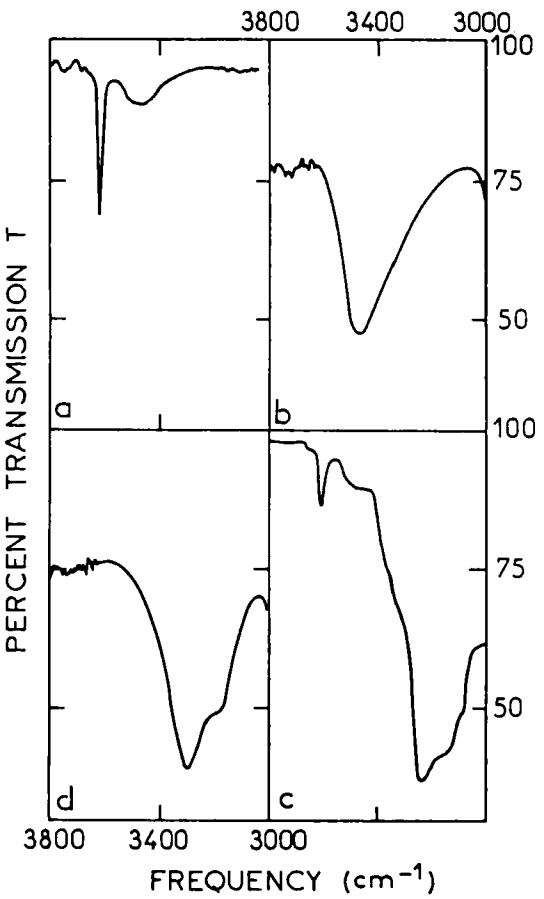

FIGURE 3 Infrared spectroscopy spectra at room temperature of compound 1 samples. Ordinates are percent transmissions T in the 3000–3800 cm^{-1} frequency range typical of O—H stretching vibration: (a) Solution C = 3.0 × 10^{-2} M, cell width = 2,00 mm; (b) crystalline powder; (c) gel phase C = 3.4 10^{-2} M, cell width = 2.70 mm; (d) xerogel.

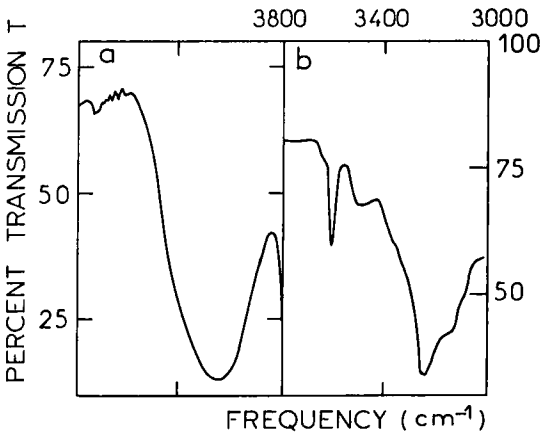

FIGURE 4 Infrared spectroscopy spectra at room temperature of compound 2 samples: (a) crystalline powder; (b) gel phase $C = 4.1 \times 10^{-2}$ M, cell width = 2.21 mm.

cm^{-1} ($\Delta\nu_{1/2} \sim 220\ cm^{-1}$) while the xerogel spectrum (Figure 3d) is very intense and even broader ($\Delta\nu_{1/2} \sim 340\ cm^{-1}$) with two maximas (3290 cm^{-1}, 3170 cm^{-1}).

For compound 2, the crystalline powder spectrum (Figure 4a) has a strong absorption at 3240 cm^{-1} ($\Delta\nu_{1/2} = 380\ cm^{-1}$) and a xerogel spectrum identical to that of compound 1.

2. Gel to xerogel transition

The filamentary organization of the gel network is strongly affected by the volume reduction of the sample[17] during solvent evaporation and mesophases are suspected as it is the case for some aqueous systems of surfactants[19] or polymeric solutions.[10] Consequently, restructuration of the gel network during the gel to xerogel transformation has been studied by polarizing optical microscopy.

Optical microscopy. When a hot droplet of a gelling steroid solution is deposited on a glass, the successive steps of gelation, steroid concentration by cyclohexane evaporation and xerogel formation are observed. Once again a distinction has to be set up when comparing compounds 1 and 2. For compound 2, as cyclohexane evaporates birefringence is enhanced and extinction crosses with black brushes and dark threads of typical Schlieren textures appear and spray over the preparation (Figure 5). Brushes in the crosses rotate in the opposite sense of the polarizing microscopic stage rotation. Following Friedel[20] the nuclei where four brushes meet are of the turning type.[21] These meeting points indicate singularities ($s = -1$). For more details concerning the analysis of the topology of singularity lines and corresponding disclinations in the structures for thermotropic systems the reader is referred to References 22, 23 and 24 for lyotropic systems. The situation is somewhat different for compound 1 for which Schlieren textures have never been observed by this way but only some droplet extinction crosses containing in an isotropic background (Figure 6).

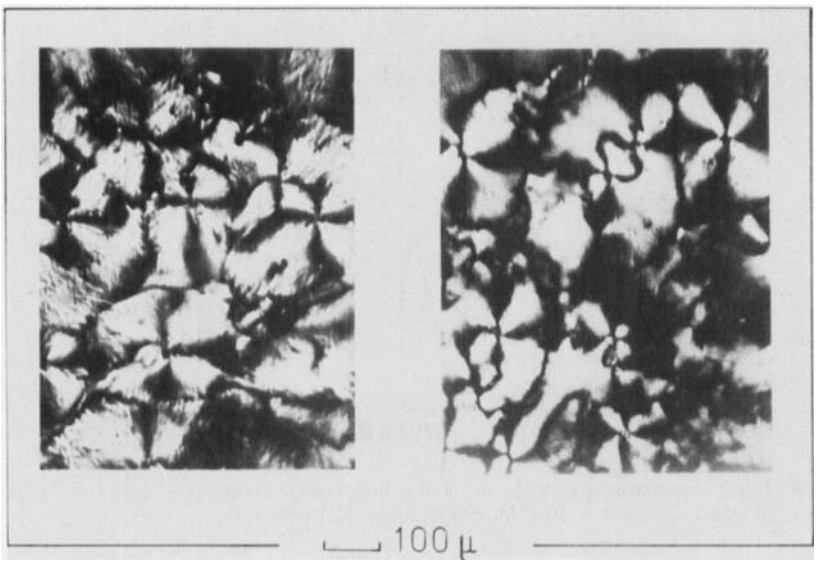

FIGURE 5 Optical textures observed during the gel to xerogel transformation of compound 2 samples. Typical Schlieren textures in birefringent domains.

Infrared spectroscopy. Further differentiation of solution, gel and xerogel states is obtained by IR spectroscopy. The solution spectrum is composed of a narrow line at 3620 cm^{-1} ($\Delta\nu_{1/2}$ = 35 cm^{-1}) and a weak broad line at 3500 cm^{-1} ($\Delta\nu_{1/2}$ = 170 cm^{-1}).

Concerning compound 1, the gel phase spectrum is made of two sets of lines. The first component is a weak solution spectrum while the second one is a very intense absorption line with two maximas (3290 cm^{-1}, 3170 cm^{-1}). In the xerogel spectrum, the solution component is absent and the spectrum appears to be an envelope of intermediate width ($\Delta\nu_{1/2} \sim 240$ cm^{-1}) of the second component gel phase spectrum (Figure 3).

For compound 2, the spectra for solution (not shown), gel phase (Figure 4b) and xerogel (not shown) are quite similar to those of compound 1.

DISCUSSION

DSC and polarizing microscopy experiments on xerogels of compound 1 indicate that the mesomorphic state obtained by solvent evaporation is transformed into a crystalline state (peaks II of Figure 1b and Table III) which in turn melts (peak I) to give the isotropic liquid at T_M. The intermediate crystalline state is obtained after an endothermic transition which transforms the xerogel in a transient more disordered state. This transition occurs simultaneously with the consecutive exothermic crystal formation (complex peak II). It is remarkable that the mesomorphic state characterized by the optical textures of Figure 5 during solvent evaporation is stable up to T_{II} temperature (391.5 K) and can only be obtained through the

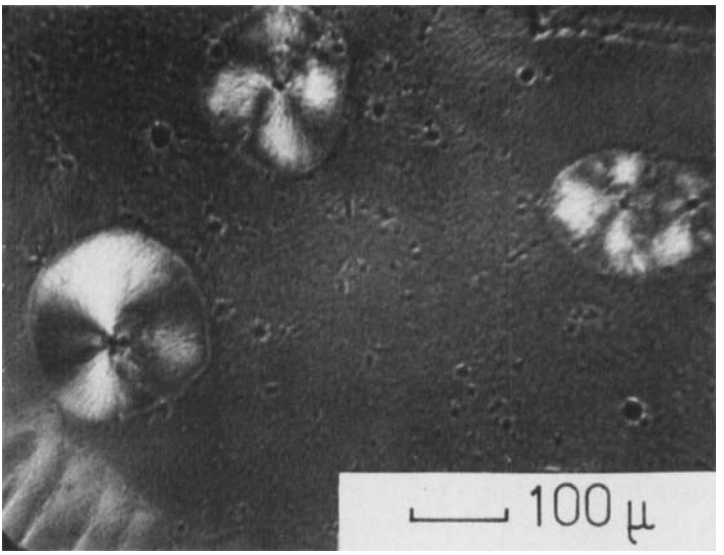

FIGURE 6 Optical textures observed during the gel to xerogel transformation of compound 1 samples. Extinction crosses are confined within droplets in isotropic medium.

compulsory solution gelation step. The related molecular structure of the xerogel is a characteristic feature of the lyotropic system which cannot exist reversibly in the solid state.

A similar conclusion is drawn from DSC traces of 12-hydroxyoctadecanoate xerogels.[4] But apart from comparison with small molecules, the same behavior is encountered in some reversible polymeric gels. As example, dried gels of isotactic polystyrene iPS[8,25] can exhibit a transformation, from an extended conformation typical of the gel phase to a threefold helical structure typical of the crystalline phase only if the gelation route is followed.

For compound 2, the first endotherm (peak III, Figure 2b1) is assigned to evaporation of some residual cyclohexane molecules (E^{760} = 353 K) participating to the structure of the network. This fact, despite identical preparation procedures, is completely absent of compound 1 thermogram (Figure 1b). The solvent participation in the structure is not yet elucidated but could occur in a different fashion for the two compounds. The second endotherm (peak II) supports the same mechanism than for compound 1 (see Figures 2b2, 2b3 and Table III) even if the exothermic crystallization (T_C) is not clearly seen by DSC.

IR spectroscopy emphasizes the short range order analogies and differences in the various states studied. The narrow 3620 cm^{-1} absorption is characteristic of the free O—H valency vibration. This absorption is strong for solutions and weak for gels demonstrating that steroid species aggregate through an hydrogen bonding mechanism. In gel phases, spectra are composed of two components: a sharp line (3620 cm^{-1}) characteristic of a steroid fraction free in solution and a broad line (3290 cm^{-1}, 3170 cm^{-1}) characteristic of a steroid fraction aggregated within the filament structures of the gel network.[18] In gels and xerogels the consequent three

dimensional multiple hydrogen bond network is responsible for the strong absorption around 3200 cm^{-1}. Similarity of xerogel and gel spectra indicates that, at the molecular level, the structure is not drastically modified by solvent evaporation. Further, gel phases spectra for compounds 1 and 2 are identical. By contrast the polycrystalline states are different as revealed by the related spectra (Figures 3b and 4a). Surprisingly a 3500 cm^{-1} absorption, relevant for some dimeric associations[26,27] is present in solution and gel phases of both compounds 1 and 2. The whole of these results suggest that the molecular organization in the gel phase filaments of both compounds is somewhat comparable to that in the polycrystalline amine (compound 2). Consequently the phase transition from the solid mesomorphic state of the xerogel to the crystalline state (peak II) occurs with a strong exothermic crystallization peak in case of compound 1 (nitroxide) where the crystallographic lattice is believed to be significantly different. In the solution, small aggregates or dimers are organized for both compounds in a comparable fashion which is reminiscent of the nitroxide (compound 1) crystalline structure as much as IR hydrogen bonding "finger print" spectra are considered. Consequently, the solvent acts only rather as a diluent for compound 1 while it is much more structurally implied for compound 2 which adopts a different configuration in solution compared to its crystalline state. Differences between the nitroxide and amine steroid derivatives are also noticed in the optical textures obtained from a concentration experiment. Typical nematic-like Schlieren textures are only seen for concentrated amine (compound 2) gel samples.

The structural sequence of Figure 7 summarizes both the concentration behavior (horizontal line) starting from a steroid solution and the thermal behavior (vertical line) starting from the solid xerogel.

Very similar optical observations have been made on gels from small amphiphilic molecules as 12-hydroxy octadecanoate derivatives[4] and from substituted urea[28] but also from lyotropic solutions of rigid polymer (poly-*p*-phenylene benzobisthiazole PBT) oriented by a spinning process.[10] In a model case of rigid rods in solution it is known that the concentration limit C** above which excluded volume effects give rise to a nematic liquid phase[29] is given by Equation (1):

$$c^{**} = M/dL^2 \tag{1}$$

where M, d and L are the rod mass, diameter and length respectively. The situation of an entangled rods solution is that of the sol phase before the gelation threshold. Previous TEM results[17] on quickly dried steroid (compound 1) sol phase solutions have shown that filaments could be approximated to finite rigid rods. Equation (1) can be combined with specific expression 2 valid in the steroid case[16] where 70 is the number of steroid molecules per rod nanometer, M_0 is the steroid molecular weight and N is the Avogadro number.

$$M = \frac{70L\ Mo}{N} \tag{2}$$

For a mean L value of 500 nm frequently encountered in the electron micrographs and a 9.5 nm rod diameter[16] an indicative C** value of 2.5×10^{-2} M is obtained.

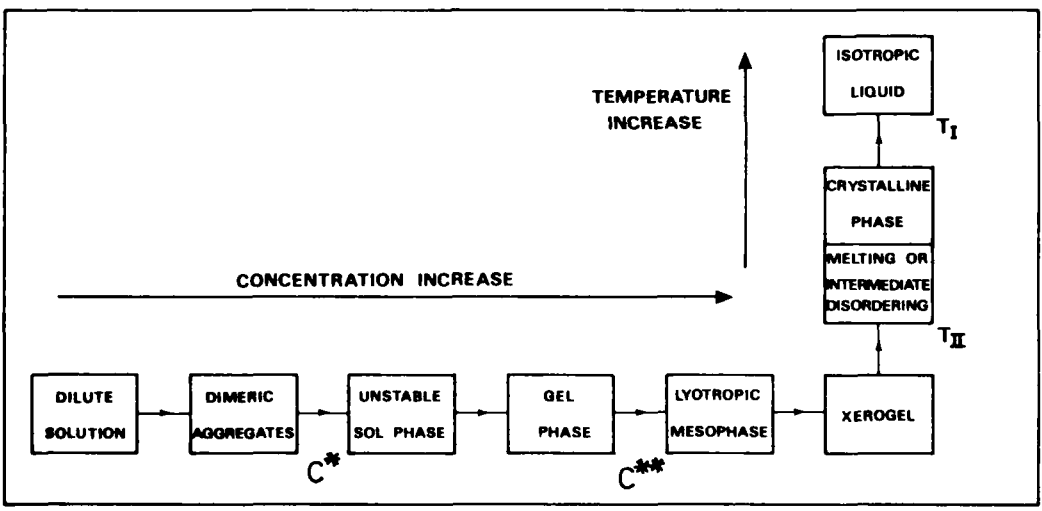

FIGURE 7 Structural sequence for steroid compounds 1 and 2 in cyclohexane solutions, gels and xerogels. Concentration dependence = horizontal arrow; temperature dependence = vertical arrow from the solid xerogel state. C* is the critical concentration for the gelation transition at a constant temperature. C** is a concentration limit for the optical observation of lyotropic mesophases.

The C** + C* value of 3.6×10^{-2} M is thus not so different from the experimental microscopic observation of enhanced birefringence around 10×10^{-2} M taking into account that a gel is made of randomly connected filaments. This may explain that anisotropic domains exist in such an evaporation process.

Additional analogies of the steroid system with thermoreversible polymeric gelling solutions could be qualitatively discussed. For instance, the regular lattice-like pattern of gel network micrographs[15] could be analyzed as resulting from a spinodal decomposition mechanism; the above mentioned reversible turbidity phenomenon could be analyzed as depending on some monotectic pseudocrystallization in solution as encountered for iPS gels[8]; the phase separation observed in magnetically oriented steroid gels[30] could confirm the existence of the coexistence curve between solvent-rich phase and oriented rigid polymer-like phase; the different thermodynamic behaviors of gel networks from compounds 1 and 2 could result from different filament network polymer-like/solvent affinities.

The reference to the Flory phase diagram for rigid rod-like polymers[31] is already considered for the above mentioned polymeric systems but also for various other polypeptides[33] and poly(γ-benzyl L-glutamate)[34] in thermoreversible gels. The present contribution on the thermoreversible gels from low molecular weight compounds reveals that the related gel network bicontinuous with the solvent-rich solution could be dependent upon the same concepts.

Acknowledgments

The author is grateful to Dr. F. Volino and R. Ramasseul for helpful discussions. I am most grateful to Dr. R. Ramasseul for having provided me with the steroid derivatives. Mr. Z. Kabsch is acknowledged for his contribution for the DSC measurements.

References

1. A. Rich and D. M. Blow, *Nature*, **182**, 423 (1958).
2. S. F. McCrea and S. Angerer, *Biochim. Biophys. Acta*, **42**, 355 (1960).
3. T. Tachibana, T. Mori and K. Hori, *Bull. Chem. Soc. Japan*, **53**, 1714 (1980).
4. T. Tachibana, T. Mori and K. Hori, *Bull. Chem. Soc. Japan*, **54**, 73 (1981).
5. A. T. Polishuk, *J. Am. Soc. Lub. Eng.*, **33**, 133 (1977).
6. P. Godard, J. J. Biebuyck, M. Daumerie, H. Naveau and J. P. Mercier, *J. Polym. Sci.*, **16**, 1817 (1978).
7. S. Waki, S. D. Harvey and A. R. Bellamy, *Biopolymers*, **21**, 1909 (1982).
8. J. M. Guenet, B. Lotz and J. C. Wittmann, *Macromolecules*, **18**, 420 (1985).
9. J. Livage, *J. Solid State Chem.*, **64**, 322 (1986).
10. H. H. Frost, Y. Cohen and E. L. Thomas, in "Reversible Polymeric Gels and Related Systems," P. S. Russo Ed., Chap. 12, ACS Symposium Series, No. 350, 1987.
11. O. Martin-Borret, R. Ramasseul and A. Rassat, *Bull. Soc. Chim. France*, II-401 (1979).
12. P. Terech, *J. Colloid Interface Sci.*, **107**, 244 (1985).
13. G. Callec, B. Gauthier-Manuel, P. Terech and R. Ramasseul, *C. R. Acad. Sci. Paris*, **293**, II-99 (1981).
14. B. Gauthier-Manuel, C. Allain and E. Guyon, *C. R. Acad. Sci. Paris*, **296**, II-217 (1983).
15. R. H. Wade, P. Terech, E. A. Hewat, R. Ramasseul and F. Volino, *J. Colloid Interface Sci.*, **114**, 442 (1986).
16. P. Terech, F. Volino and R. Ramasseul, *J. Phys. France*, **46**, 895 (1985).
17. P. Terech and R. H. Wade, accepted in *J. Colloid Interface Sci.*

18. P. Terech, R. Ramasseul and F. Volino, *J. Colloid Interface Sci.*, **91**, 280 (1983).
19. V. Luzzati, H. Mustacchi, A. Skoulios and F. Husson, *Acta Cryst.*, **13**, 660 (1960).
20. G. Friedel, *Ann. Phys.* (Leipzig), **18**, 273 (1922).
21. G. W. Gray and P. A. Winsor in "Liquid Crystals and Plastic Crystals," Vol. 2, Chapter 2, 25 N. H. Hartshorne "Optical properties of liquid crystals," Ellis Horwood Ltd., Chichester (1974).
22. D. Demus and L. Richter in "Textures of Liquid Crystals," Verlag Chemie, New York (1978).
23. F. Lachampt and R. M. Vila, Revue Française des Corps Gras, **2**, 87 (1969).
24. F. B. Rosevear, *J. Soc. Cosmetic Chemists*, **19**, 581 (1968).
25. P. R. Sundararajan, N. Tyrer and T. Bluhm, *Polym. Bull.*, **6**, 285 (1982).
26. F. S. Parker and K. R. Bhashkar, *Biochemistry*, **7**, 1286 (1968).
27. J. J. Feher, L. D. Wright and D. B. McCormick, *J. Phys. Chem.*, **78**, 250 (1974).
28. N. S. Murthy, Proceedings IUPAC, Amherst, 833 (1982).
29. J. Torbet, J. M. Freyssinet and G. Hudry-Clergeon, *Nature*, **289**, 91 (1981).
30. To be published.
31. P. J. Flory, *Proc. Roy. Soc.*, **A234**, 73 (1956).
32. P. G. de Gennes in "Scaling Concepts in Polymer Physics," Chap. V, p. 128, Cornell Univ. Press, Ithaca, 1980.
33. K. Tohyama and W. G. Miller, *Nature*, **289**, 813 (1981).
34. S. Sasaki, M. Hikata, C. Shiraki and I. Uematsu, *Polymer J.*, **14**, 205 (1982).